Iranian Journal of Science and Technology, Transactions of Civil Engineering
https://doi.org/10.1007/s40996-022-00946-2

RESEARCH PAPER

Numerical Study of the Variation of the Voids Ratio of Soil Improved Stone Column

Amal Mekaoussi[1] · Toufik Karech[1] · Abdelkader Noui[1]

Received: 21 January 2022 / Accepted: 2 August 2022

Abstract

This research work is part of the trend of soil reinforcement procedures aimed at improving poor quality soils. Among these techniques, those that use stone columns. Although the aspects concerning the construction processes are now well mastered, the design methods of these reinforced soils remain to be developed.

A numerical simulation presented to study two unit cell models. The 3D proposed simulation model is subjected to gravity and a static load. The first model presents a unit cell composed of stone column in the center and a surrounding clay soil volume. The second is converted into an equivalent unit cell (the volume averaging) in terms of physical and mechanical parameters of a composite material (equivalent parameters).

Under the effect of incrementally loading–unloading applied to these unit cell models, voids ratio variations and stress path evolution are analyzed. The results indicate that applying a load to an equivalent unit cell can affect the void ratio-volumetric deformation curves and increase settlement. The void ratio and the corresponding volumetric deformation decreased by comparing the equivalent homogenized model with the non-homogenized model. The results show that the void ratio decreases by about 10% on average, but the volumetric strain decreases by 80%. Therefore, the stress path corresponding to the decrease of the average effective stress by 1% increases the deviatoric stress on average by 10%. Diagrams obtained by numerical results are in accordance with the results derived from experimental observations. The adopted technique can substantially can describe sufficiently the influence of the equivalents physical and mechanical parameters on the improvement in the soil of unit cell.

Keywords Stone column · Clay soil · Equivalent parameters · Equivalent unit cell · Void ratio · Stress path

1 Introduction

Soils improved by stone column are composite soils constituted of granular material and loose soil. The behavior of these composite soils is not well controlled, due to their non-homogeneous structural matrix. Many research studies have been conducted to investigate the performance of composite soils, and a number of researchers have adopted the unit cell concept in their analysis (Babu et al. 2013; Killeen and McCabe 2014; Maheshwari and Khatri 2012; Ng and Tan 2014a; Shahrour and Pruchinikcki 1991).

The unit cell concept is a simple idea adopted for composite soils, to model an infinite number of conditions of a group of stone columns. This conditions may be inadequate only in some cases researchers noted that the assumptions made in the unit cell concept are valid only for rigid rafts and that the assumptions appear to be significant weaknesses with regard to the boundary conditions (Schweiger and Pande 1986). For constituents of reinforced soil (Abdelkrim and Buhan 2007; Buhan et al. 1989; Gueguin et al. 2013, 2015; Hassen et al. 2010, 2013; Jellali et al. 2007, 2005). Several authors adopted the unit cell model (UCM Study of behavior of foundations on soil reinforced by stone columns relies first, on the verification of bearing capacity and second, on the settlement predictions (Bouassida and Carter 2014).

Numerous contributions were proposed to predict the settlement of foundations on soil reinforced by stone columns. Different modeling and various constitutive laws were adopted for the predictions of bearing capacity and settlement of column-reinforced foundations (Castro 2017;

✉ Amal Mekaoussi
amel.mekaoussi@univ-batna2.dz

[1] Department of Civil Engineering, Faculty of Technology, University Batna 2, 05078 Batna, Algeria

Published online: 29 August 2022

Ellouse et al. 2016; Noui et al. 2019; Tabchouche et al. 2019). Despite the intensive practice of the UCM, considered by several authors, since the last decade a big interest was accorded to perform numerical modeling of reinforced soil. Therefore, the homogenization technique has been developed to model stone column improved grounds by establishing the equivalent material properties for the composite ground. However, homogenization techniques based on the elasto-plastic behavior of the constituent materials found in the literature require modification in terms of the finite element constitutive models which are difficult for practical engineers to apply. Therefore, a simple yet effective way of predicting the performance of stone column improved grounds has been invoked in this study.

A new for the design method for reinforced soil structures, based on the theory of failure computation intended as a generalization of limit analysis, on the theories of homogenization of periodic heterogeneous media and in particular the application to soils reinforced with stone columns (Buhan et al. 1989) by establishing the equivalent properties of materials for composite soil.

An idea was introduced, to analysis the behavior of soils improved by stone columns. This idea consists in using the volume averaging approach (equivalent homogeneous soil with improved properties) (Castro 2017; Hadri et al. 2021; Laouche et al. 2021; Ng and Tan 2015). Two similar models of unit cell were studied. One is a unit cell of the stone column surrounding the clay soil, and the other is an equivalent model of these physical and mechanical parameters. A simple equivalent method is developed in this study to obtain equivalent properties of the equivalent soil (equivalent: stiffness, cohesion, friction angle, and unit weight). These equivalent properties are then easily introduced into Plaxis 3D code for a numerical analysis.

2 Review of Related Works

A few researchers have proposed some formulations for simplified homogenization method of the composite soil. This section briefly introduces their methods.

Nazir and Azzam (2010) presents the results of laboratory model tests for studying the improvement in soft clay layer by using both partially replaced sand piles with/without confinement. The effect of sand pile to improve the bearing capacity and to control the settlement. The results show that the improvement in load bearing capacity is remarkable; using both partially replaced sand pile with and without confinement by skirts.

Therefore, the bearing capacity failure mechanism of a footing rested on soft clay can be modified from exclusive settlement to general bearing capacity failure at the tip of confined replaced sand column.

Ng and Tan (2014a) developed a homogenization technique to model stone column improved soils, by establishing the equivalent material properties for the composite soil. A simple and effective method of predicting the performance of stone column improved grounds invoked in this study. This approach is called the equivalent column method (ECM). Authors provide equivalents stiffness and permeability for the composite material. The method is derived from an analysis by using the unit cell model in a 2D finite element axisymmetrical model. The settlement is calculated and a correction factor is obtained via a comparison with the results calculated using a single averaging composite stiffness for the improved ground.

$$E_{\text{composite}} = \alpha E_{\text{c}} + (1-\alpha)E_{\text{s}} \tag{1}$$

where α: area replacement ratio $\left(\alpha = {}^{A_c}\!/_{A}\right)$; A_{c}: area of the stone column; A = total influence area. E_{c} stiffness of the column, and E_{s} stiffness of the surrounding soil.

$$E_{\text{eq}} = \frac{E_{\text{composite}}}{N_{\text{corr}}} \tag{2}$$

$$N_{\text{corr}} = \frac{E_{\text{composite}}}{E} \tag{3}$$

N_{corr}: the ratio of the composite stiffness over the calculated stiffness E.

Castro (2017) reviewed the main modeling techniques for stone columns and also the homogenization method. It consists in replacing the stone columns and the soft soil by an equivalent homogeneous soil with improved properties. This equivalent homogeneous soil occupies the zone treated with stone columns. This model simplifies enormously the geometry of the problem. For example, when the problem itself has a highly complex geometry and the zone treated with columns is just a part of the problem, this method is highly advisable. For the design stage, this method allows the area replacement ratio $\left(a_{\text{r}}\right)$ to be varied without changing the geometry of the model, just the material parameters. The most straightforward proposal for obtaining the improved parameters of the equivalent homogeneous soil is just to average the soil and column parameters weighted by their corresponding areas though ar. Thus, for the elastic modulus, the weighted average is:

$$E_m = E_{\text{s}}\left(1 - a_{\text{r}}\right) + E_{\text{c}} a_{\text{r}} \tag{4}$$

A more detailed analysis shows that the equivalent homogenous soil should be anisotropic by nature to account for the column orientation.

Zeydi and Boushehrian (2019) studied the behavior of circular shallow footings on soft clay soils with skirted and non-skirted sand piles. Different piles with varying length to clay layer thickness ratios ranging from 0.25 to 1 were modeled experimentally, as well as numerically, both with and without skirt. The results founded indicate that the use of skirted piles can affect the load–settlement curves and increase the bearing capacity. By increasing the ratio of pile length to clay thickness, the bearing capacity of the shallow foundation will be increased and the corresponding settlement will be decreased. Therefore, the bearing capacity failure mechanism of a footing resting on soft clay can be modified from the punching failure to the general shear failure at the tip of the confined replaced sand column. Load–settlement diagrams and bearing capacity obtained by numerical results are in accordance with the results derived from experimental observations.

Hamzh et al. (2019) investigated the effect of dual diameter stone column of various length and diameter ratios on bearing capacity of soft soil. The method (larger diameter at the top and smaller diameter at the lower column) demonstrated the possibility of using smaller volume of stone material and hence less cost but at the same time able to perform similar capacity to the standard column. A design chart is supplemented to determine the optimum geometry of the stone column. The failure mechanism of the non-uniform-shaped columns generally comprised of both punching and bulging, although for the diameter ratio = 1:5, only punching failure was observed. The results presented in this paper are limited to soft clay properties which are assumed homogenous and with a fixed ratio of stone-soil stiffness. For cases like layered soils, stiffness increases with depth, different column stiffness, it is likely that the numerical results differ significantly and require new sets of numerical simulations and investigation.

Laouche et al. (2021) investigated of the behavior of a reduced model of a reinforced soil massif by a sand column tested in the laboratory. These tests involved the installation of sand columns in clay by different methods (with the soil replacement method and with compacting of the columns). The first part of this investigates aims to study the effect of the intensity of the compaction stress of the sand columns on the surrounding soil and the effect on the behavior of the soil-column massif. In the second part, a sand column was installed by two methods: one with replacement of the soil and without compaction and the other with displacement of the soil. A comparison between the two methods has been established. By determining the equivalent characteristics for the soil-column massif, this study made it possible to characterize the effect of the installation method of the columns on the settlements, the void ratio e of kaolin, the equivalent void ratio e_{eq} of the massif soil-column and on the compressibility parameters of the massif (equivalent compression index C_{ceq} and swelling index C_{seq}), by comparing the results obtained with those of the unreinforced soils that constitute the reference case.

$$\frac{\Delta V}{V_0} = \frac{\Delta e}{1 + e_0} \tag{5}$$

$$a_s = {}^{A_{\mathrm{col}}}\!/\!{}_{A_{\mathrm{mol}}} \tag{6}$$

$$e_{\mathrm{eq0}} = e_{\mathrm{sa}}a + e_{\mathrm{ka}}(1 - a) \tag{7}$$

$$C_{\mathrm{ccal}} = C_{\mathrm{csa}}a + C_{\mathrm{Cka}}(1 - a) \tag{8}$$

$$C_{\mathrm{scal}} = C_{\mathrm{ssa}}a + C_{\mathrm{ska}}(1 - a) \tag{9}$$

where C_{ccal}: calculated equivalent compression index of the massif; C_{csa}: compression index of the sand column; *C*cka: kaolin compression index; C_{sca}l: calculated equivalent swelling index of the massif; C_{ssa}: swelling index of the sand column; C_{ska}: kaolin swelling index; The results obtained showed that the techniques used for the installation of columns have significant effects on the behavior of reinforced massifs.

Hadri et al. (2021) reported a case of loose soil with high compressibility, treated with stone column technique. The case history was studied using a two-dimensional finite element model to simulate the behavior of stone columns under loads. The numerical study was performed using the unit cell approach. The elastic-perfectly plastic Mohr–Coulomb behavior was adopted for the soil and column. The numerical results of the settlements were compared with the field measurements collected from the case history, which showed good agreement. The equivalent area method was used and verified in this study. The equivalent area method yields similar values to field measurements.

$$\gamma_{\mathrm{eq}} = \gamma_{\mathrm{c}}a_s + \gamma_{\mathrm{s}}\left(1 - a_s\right) \tag{10}$$

$$\varphi_{\mathrm{eq}} = \tan^{-1}\left(\tan\varphi_{\mathrm{c}}a_s + \tan\varphi_{\mathrm{s}}\left(1 - a_s\right)\right) \tag{11}$$

$$C_{\mathrm{eq}} = C_{\mathrm{c}}a_s + C_{\mathrm{s}}\left(1 - a_s\right) \tag{12}$$

$$E_{\mathrm{eq}} = E_{\mathrm{c}}a_s + E_{\mathrm{s}}\left(1 - a_s\right) \tag{13}$$

a_s is the area replacement ratio $a_s = {}^{A_{\mathrm{c}}}\!/\!{}_{A}$; A_{c}: area of the stone column, A: total influence area.

This investigation also examined the effect of various parameters, including column material stiffness, stone column diameter, columns spacing and embankment height. The results of the parametric study with the unit cell approach showed good agreement with the equivalent area method for predicting settlement.

3 Equivalent Homogenous Soil

In this section, the concept of the equivalent homogenous soil is described. The purpose of the soil-columns equivalent system is the determination of the composite soil parameters for the Mohr–Coulomb model. Unit cell principal is proposed to modeling stone columns surrounding clay soil and distributed loads coming from a large structure. The stone columns are considered sufficiently close to each other and frequently distributed in a regular mesh.

In this analysis, the ratio of the total area of stone column in the area of the unit cell and the equivalent rigidity. This is done in order to calculate the cohesion, friction angle and unit weight of the reinforced soil. The most basic proposal, to obtain the improved parameters of an equivalent soil, is to compute the average the soil and column parameters calculated using their corresponding areas. It should be noted that the equivalent unit cell presents the same geometric characteristics as the initial unit cell (Fig. 1).

The properties of the clay soil and the stone column are improved in terms of their physical and mechanical parameters according to the following formulas:

$$a = \frac{A_c}{A} \tag{14}$$

$$E_{equiv} = aE_c + (1-a)E_s \tag{15}$$

$$C_{equiv} = aC_c + (1-a)C_s \tag{16}$$

$$\varphi_{equiv} = a\varphi_c + (1-a)\varphi_s \tag{17}$$

$$\gamma_{equiv} = a\gamma_c + (1-a)\gamma_s \tag{18}$$

where, a: area replacement ratio (area of stone column over area of total unit cell); A_c: area of stone column; A: total area of unit cell; E_{equiv}, E_c, E_s: rigidity of equivalent model, stone column and clayey soil, respectively; C_{equiv}, C_c, C_s: cohesion of equivalent model, stone column and clayey soil, respectively; φ_{equiv}, φ_c, φ_s: friction angle of equivalent model, stone column and clayey soil, respectively; γ_{equiv}, γ_c, γ_s: unit weight of equivalent model, stone column and clayey soil, respectively.

4 Numerical Simulation

Plaxis 3D finite element software is used in this research study to analysis the behavior of two-unit cell models. The first one is composed of stone column surrounded by soil (non-homogenized unit cell) and the second is homogenized in terms of its physical and mechanical parameters (equivalent materials) computed by the volume average method, given the formulae (14–18).

4.1 Assumptions, Model Geometry and Material Properties

Assumptions are considered in the numerical calculation:

- The constitutive law used for soft soil and stone column is Mohr–Coulomb's law;
- The constitutive law used for the distribution massif and concrete is that of linear elasticity;
- The initial vertical stress due to the gravity load is considered in the analysis;

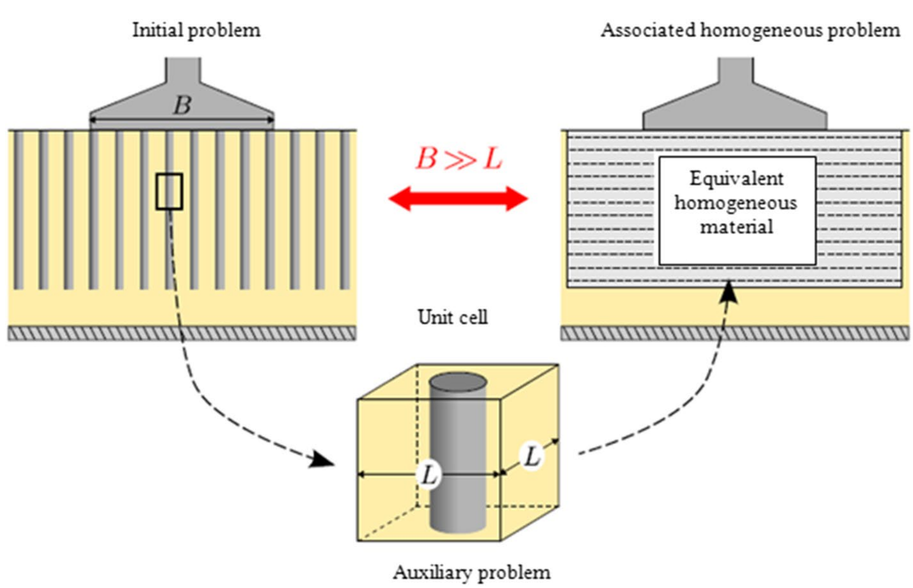

Fig. 1 Principle of the equivalent homogenous material applied to unit cell (Gueguin, 2015)

- The stress due to the installation of the stone column depends on the method of implementation.

To achieve the above hypotheses, the following geometric model is used for the analysis. The unit cell is a plane square of 2 m and of depth $L=20$ m, the diameter of the stone column is $D=100$ Cm and the soil layer is homogeneous (Fig. 2). The unit cell is always topped by a 50 cm thick of distribution mattress and the latter supports a 20 cm thick concrete slab. An incremental loading–unloading of 5 KN/m^2 is applied at the top of unit cell (50 KN/m^2 to 80 KN/m^2). In this case, during the setting up the column element, the top and bottom faces of the model are blocked by rigid walls to simulate the vertical confinement of a deep layer.

4.1.1 Properties of Materials

The stone column and the soft soil display both an Elastic–Plastic behavior (Mohr–Coulomb model). Furthermore, the mattress and the raft exhibit linear elastic behavior. The soft soil is considered to represent the compressed soil. The Geotechnical characteristics of the soft soil, stone column, mattress and concrete slab materials are summarized in Table 1.

4.2 Type of Model, Choice of Elements, Boundary Conditions and Mesh

The model presented in 3D numerical simulation is considered as a representative of a unit cell. It constitutes of triangular elements with 15 nodes. Displacement boundary

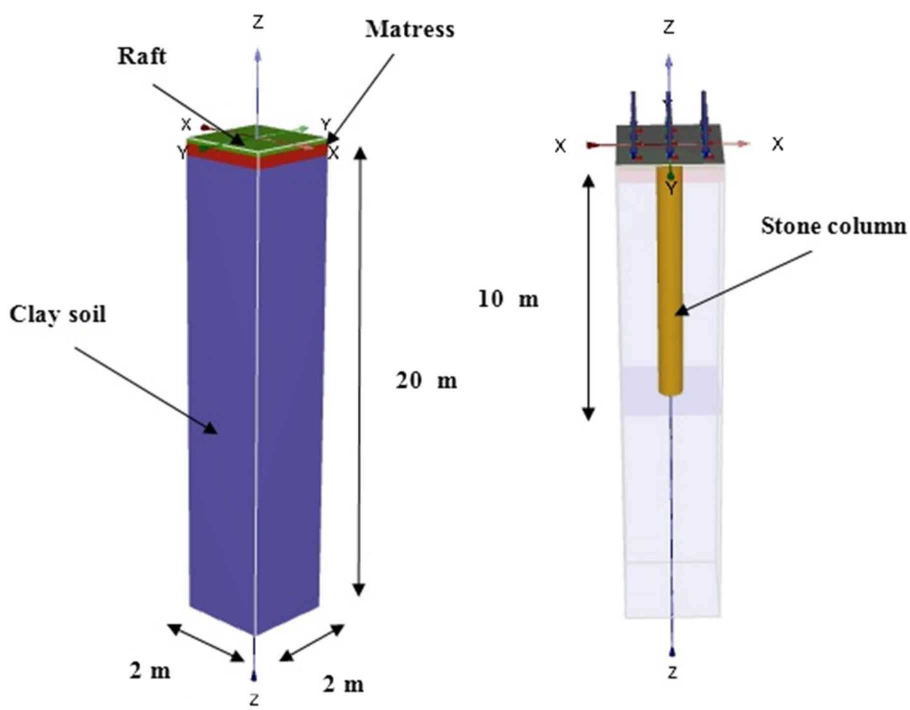

Fig. 2 Model geometry of unit cell

Table 1 Geotechnical characteristics of materials of the components of the unit cells

Identification	Parameters	Concrete	Mattress	Unit cell		Equiv unit cell	Unit
				Stone column	Clay soil	Equivalent soil	
Behavior	Type	Linear- elastic	Linear-elastic	(M.C) Drained	(M.C) Undrained	(M.C) Drained	/
Soil weight	γ_{sat}	25	23	23	17	16	kN/m^3
Young's modulus	E_{ref}	30 000	60 000	50 000	2 000	11 600	k Pa
Poisson's ratio	ν	0.20	0.25	0.25	0.33	0.33	/
Cohesion	C_{ref}	/	/	1	5	4.2	k Pa
Friction angle	φ	/	/	38	25	28	°
Dilatancy angle	ψ	/	/	8	0	0	°

conditions are fixed for all lateral sides of the unit cell. Table 2 summarizes and specifies the type of analyzed models.

4.3 Methods and Phases of Calculation

PLAXIS 3D Foundation computer package is used to simulate two models of unit cell. Each one of them is depicted in thirteen phases. The first seven phases correspond to an increment of 5 kPa of loading from 50 to 80 kPa, and the last six phases represent an incremental unloading with the same computing step.

4.3.1 Characteristic Points Chosen for the Analysis

(B, E, H) are points chosen as the interface between the stone column and the surrounding soft soil (heterogeneous model). These same positions of points are denoted by points *(b, e, h)* in the equivalent unit cell (homogenous model). In order to get an overview of the unit cell behavior, other characteristic points *(C, F, I)* are selected at the outer boundary of the stone column and the soft soil unit cell. These same positions are also designated as points *(c, f, i)* for the equivalent unit cell (Fig. 3).

Table 2 Models analyzed in both type of simulation

Type of simulation	Models	Specifications
Non-homogenized unit cell	Point (B)	At the top of stone column and close to the stone column soil interface
	Point (E)	At the middle of stone column and close to the stone column soil interface
	Point (H)	At the bottoms of stone column and close to the stone column soil interface
	Point (C)	At the top and at the outer boundary of non-homogenous unit cell
	Point (F)	At the middle and at the outer boundary of non-homogenous unit cell
	Point (I)	At the bottom and at the outer boundary of non-homogenous unit cell
Homogenized unit cell	Point (b)	At the top of the homogeneous unit cell
	Point (e)	At the middle of the homogeneous unit cell
	Point (h)	At the bottom of the homogeneous unit cell
	Point (c)	At the top and at the outer boundary of unit cell
	Point (f)	At the middle and at the outer boundary of unit cell
	Point (i)	At the bottom and at the outer boundary of unit cell

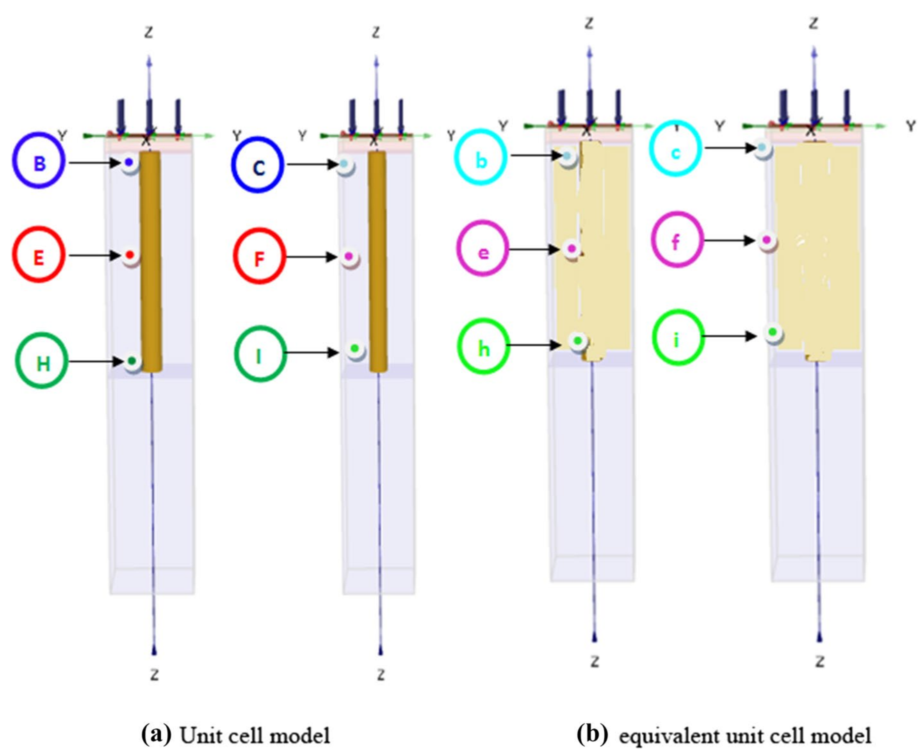

Fig. 3 Presentation of the analysis points

5 Results and Discussion

5.1 Analysis of the Variation of the Void Ratio as a Function of Volumetric Deformation

The voids ratio indicates the compactness of the granular arrangement of a soil. A low void ratio corresponds to a low void in the soil, and thus corresponds to a compact particle arrangement. The overall void ratio in the case of a heterogeneous soil raises a problem of representativeness. Indeed, the calculation to be performed requires the dry density of the soil and that of the particles it contains (Fig. 4).

By comparing the behavior of the homogeneous unit cell to the non-homogeneous cell, one can distinguish the following:

- The further away one is from the effect of the overload, the more the values of the volume deformation (ε_v) and the values of the voids ratio (e) decrease for both cells.
- Whether near or far from the stone column gave almost the same results (the comparison is made between the same positions of the non-homogeneous model and the homogeneous model).

  Almost identical values are recorded for the same positions close or far from, the column according to Tables 2 and 3 and the following is noted:
- The rate of decrease in the values of the volume deformation (ε_v) of the homogeneous model compared to the non-homogeneous model is very important 80% see (Table 5).
- The rate of decrease in the values of the voids ratio (e) of the homogeneous model compared to the non-homogeneous model is in the following increasing order: 5%, 9%, 14% see (Table 5).

For the homogeneous model, the values found in the loading phases are inversely proportional to those found in the unloading phases. This is not the case for the non-homogeneous model.

Table 4 below summarizes the results of the rate of change of the volume deformation and the voids ratio of the homogeneous model compared to the non-homogeneous model (Fig. 5)

5.2 Analysis of Variation of Deviatoric Stress as a Function of Effective Means Stress (Stress Path)

Soils have a particularly complex behavioral law. For an isotropic soil, the stress path is vertical and represents undrained shear. In contrast, nonlinear behavior leads to nonlinear and irreversible deformation.

The stress path is broken in the direction of increasing mean pressures. The ultimate state is reached at low material deformation. To show the effect of the stone column on the behavior of the unit cell, a stress path has been studied for points *B, E, H* as well as points *C, F, I* of the non-homogenized cell model (Fig. 6) and others *b, e, h* and *c, f, i* of the homogenized cell model (Fig. 7). Moving away from the applied overload, an increase in the values of the stress deviator of the non-homogenized and homogenized model is observed.

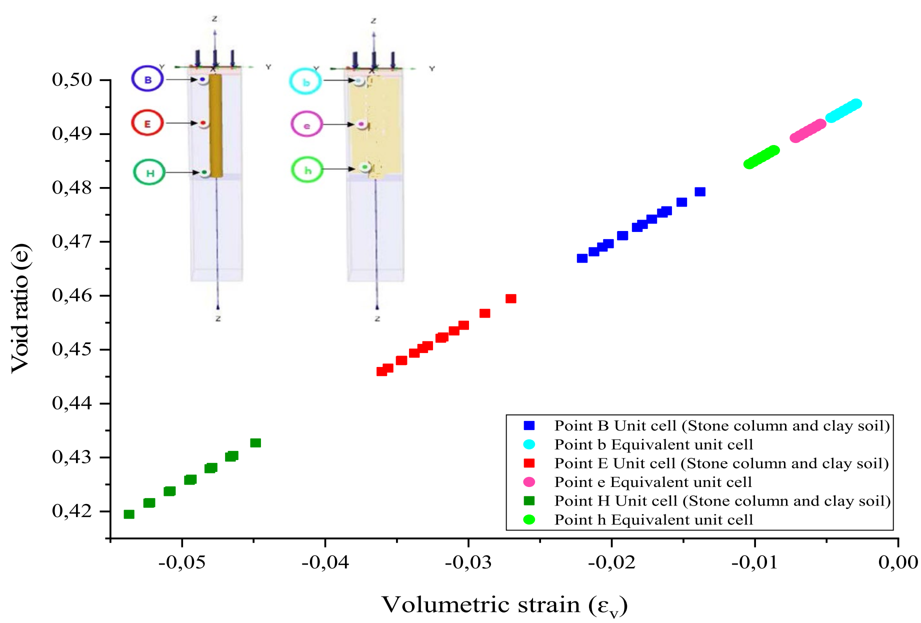

Fig. 4 Variation in void ratio between the interface of the column and the surrounding soil

Table 3 Results of variation of the voids ratio as a function of the volumetric deformation according to the different loading–unloading phases

Point B		Point b		Point E		Point e		Point H		Point h	
Unit cell		Equiv Unit cell		Unit cell		Equiv Unit cell		Unit cell		Equiv Unit cell	
ε_v [10^{-3}]	e [10^{-3}]	ε_v [10^{-3}]	e [10^{-3}]	ε_v [10^{-3}]	e [10^{-3}]	ε_v [10^{-3}]	e [10^{-3}]	ε_v [10^{-3}]	e [10^{-3}]	ε_v [10^{-3}]	e [10^{-3}]
−13,829	479,256	−2936	495,597	−27,032	459,452	−5432	491,852	−44,860	432,710	−8684	486,975
−15,101	477,349	−3224	495,163	−28,846	456,731	−5719	491,422	−46,427	430,359	−8968	486,548
−16,455	475,318	−3513	494,730	−30,327	454,509	−6006	490,991	−47,896	428,155	−9253	486,121
−17,852	473,222	−3802	494,297	−31,770	452,345	−6293	490,561	−49,353	425,971	−9537	485,695
−19,257	471,114	−4090	493,865	−33,197	450,204	−6579	490,131	−50,803	423,795	−9821	485,269
−20,649	469,027	−4378	493,433	−34,656	448,016	−6865	489,702	−52,250	421,624	−10,105	484,843
−22,052	466,922	−4666	493,001	−36,043	445,935	−7152	489,273	−53,697	419,455	−10,389	484,417
−21,235	468,147	−4378	493,433	−35,611	446,584	−6865	489,702	−52,318	421,523	−10,105	484,843
−20,231	469,653	−4090	493,865	−34,694	447,960	−6579	490,131	−50,900	423,650	−9821	485,269
−19,225	471,162	−3802	494,297	−33,775	449,338	−6292	490,561	−49,478	425,924	−9537	485,695
−18,218	472,673	−3513	494,730	−32,854	450,719	−6006	490,991	−48,051	427,924	−9253	486,121
−17,206	474,191	−3224	495,163	−31,931	452,103	−5719	491,422	−46,619	430,071	−8968	486,548
−16,164	475,754	−2936	495,597	−31,006	453,492	−5432	491,852	−45,183	432,225	−8683	486,975

Points located at the interface between the stone column and the surrounding soil

Table 4 Results of variation of the voids ratio as a function of the volumetric deformation according to the different loading–unloading phases

Point C		Point c		Point F		Point f		Point I		Point i	
Unit cell		Equiv unit cell		Unit cell		Equiv unit cell		Unit cell		Equiv unit cell	
ε_v [10^{-3}]	e [10^{-3}]	ε_v [10^{-3}]	e [10^{-3}]	ε_v [10^{-3}]	e [10^{-3}]	ε_v [10^{-3}]	e [10^{-3}]	ε_v [10^{-3}]	e [10^{-3}]	ε_v [10^{-3}]	e [10^{-3}]
−13,874	479,189	−2933	495,601	−26,916	459,627	−5413	491,880	−44,281	433,578	−8701	486,949
−15,321	477,018	−3222	495,167	−28,729	456,907	−5700	491,449	−45,965	431,052	−8985	486,522
−16,745	474,883	−3510	494,734	−30,197	454,704	−5987	491,019	−47,444	428,835	−9270	486,095
−18,177	472,734	−3799	494,301	−31,633	452,550	−6274	490,589	−50,312	426,675	−9554	485,669
−19,608	470,588	−4087	493,869	−33,055	450,417	−6561	490,159	−50,803	424,532	−9838	485,243
−21,048	468,428	−376	493,437	−34,509	448,237	−6847	489,729	−51,741	422,389	−10,122	484,817
−22,458	466,312	−4664	493,005	−35,893	446,160	−7133	489,300	−53,156	420,265	−10,406	484,391
−21,826	467,261	−4376	493,437	−35,499	446,827	−6847	489,729	−51,891	422,164	−10,122	484,817
−20,868	468,698	−4087	493,869	−34,529	447,207	−6561	490,159	−50,544	424,185	−9838	485,243
−19,908	470,138	−3799	494,301	−33,607	449,589	−6274	490,589	−49,192	426,212	−9554	485,669
−18,947	471,580	−3510	494,734	−32,683	450,975	−5987	491,019	−47,837	428,345	−9270	486,095
−17,982	473,027	−3222	495,167	−31,758	452,363	−5700	491,449	−46,477	430,284	−8985	486,522
−17,005	474,493	−2933	495,601	−30,829	453,756	−5413	491,880	−45,113	432,330	−8701	486,949

Points located at the outer limit of the unit cell

The comparison between the behavior of the equivalent unit cell model and the unit cell model (stone column and soft soil) leads to the following observations:

- For both studied models, the further away from the effect of the overload applied to the unit cell, the more the values of the effective mean stress (p') decrease, meanwhile the values of the deviatory stress q increase.
- The proximity or distance from the stone column gave almost the same results (the comparison is made between the same positions of the unit cell model

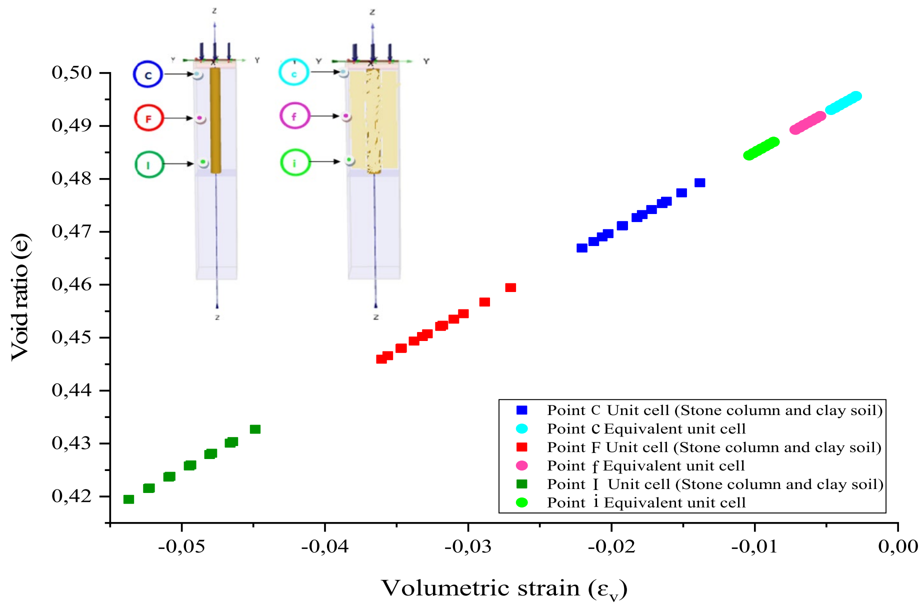

Fig. 5 Variation of the void ratio of the points at the outer end of the unit cell

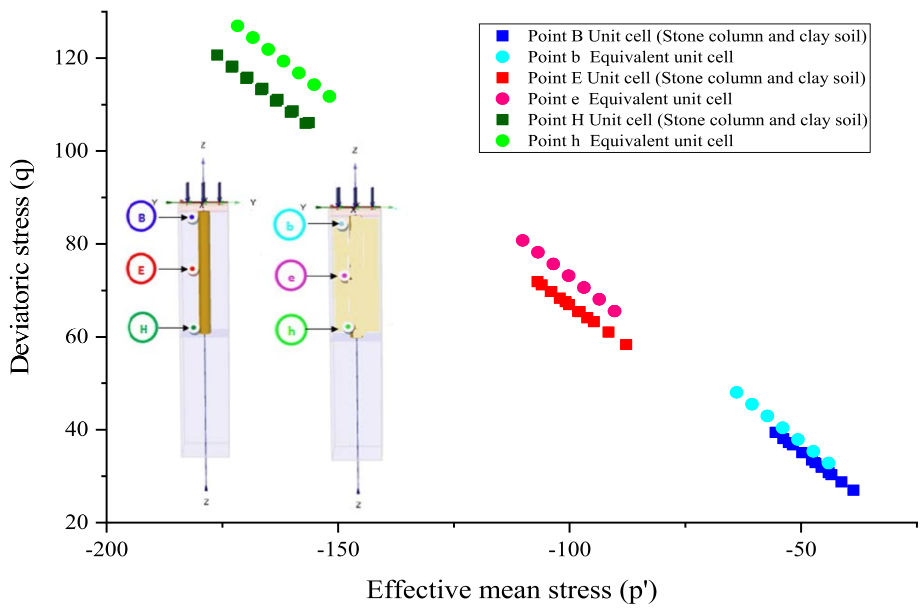

Fig. 6 Variation of the stress path of the points of the between the interface of the column and the surrounding ground

(stone column and soft soil) and then the model of an equivalent unit cell.

Almost identical values are recorded for the same positions close or far from the column according to Tables 5 and 6 and noted below:

- The rate of decrease in the values of the effective mean stress (p') of the equivalent model compared to the model of unit cell (stone column and soft soil) is very low 1% and even null.
- The rate of increase in the values of the deviatory stress (q) of the equivalent unit cell model in relation to the unit cell model is in the following decreasing order: 20%, 10%, 5% (Table 7).

Table 8 summarizes the results rates of variation (p') and (q) of the model of equivalent unit cell compared to the model of unit cell (stone column and soft soil).

Laouche et al. (2021) present an experimental study focuses in the investigation of the behavior of a reduced model of soil (Kaolin) reinforced by a stone column (Sand). The objective this study is to characterize the effect of the compaction stress of the sand columns on surrounding soil and on the behavior of the reinforced soil massif. For this, sand columns of the same diameter (20 mm) were installed by the method with Replacement of the soil and with Compaction (WR-WC). They were

Fig. 7 Variation of the stress path of the points of the points at the outer end of the unit cell

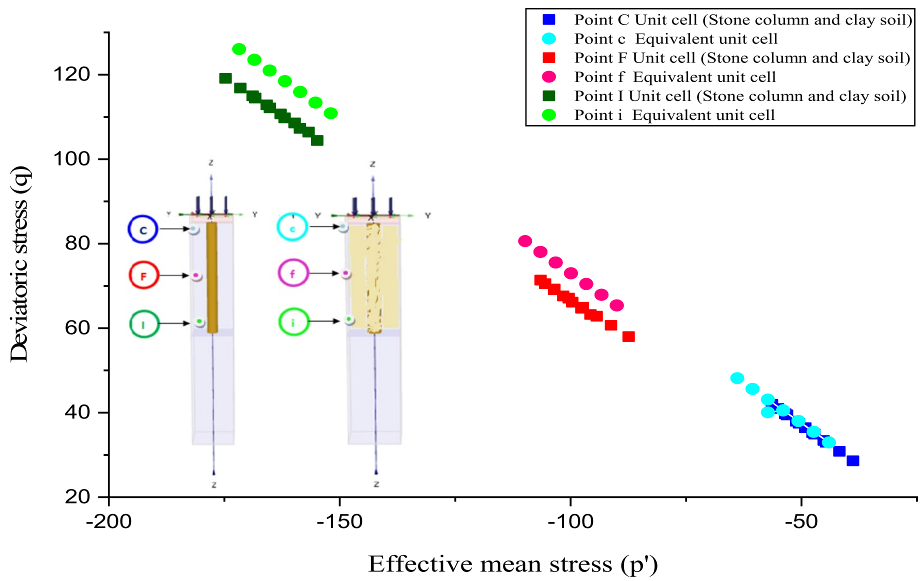

Table 5 Summarizes the rate of variation of volume deformation and void ratio of the two models

Equivalent unit cell model- unit cell model)	Rate of variation					
	B-b	E-e	H-h	C-c	F-f	I-i
Volumetric deformation (ε_v)	80%	81%	81%	80%	81%	81%
Void ratio (e)	5%	9%	14%	5%	9%	14%

Table 6 Results of variation of deviatory stress q and effective mean stress p' according to the different loading–unloading phases

Point B		Point b		Point E		Point e		Point H		Point h	
Unit cell		Equiv Unit cell		Unit cell		Equiv Unit cell		Unit cell		Equiv Unit cell	
p' [kN/m^2]	*q* [kN/m^2]	*p'* [kN/m^2]	*q* [kN/m^2]	*p'* [kN/m^2]	*q* [kN/m^2]	*p'* [kN/m^2]	*q* [kN/m^2]	*p'* [kN/m^2]	*q* [kN/m^2]	*p'* [kN/m^2]	*q* [kN/m^2]
−38,719	26,983	−44,061	32,819	−87,779	58,342	−90,295	65,546	−156,322	106,107	−151,848	111,748
−41,300	28,750	−47,370	35,357	−91,608	61,036	−93,605	68,081	−159,809	108,650	−155,158	114,283
−44,056	30,784	−50,678	37,894	−94,746	63,226	−96,914	70,615	−163,081	111,097	−158,467	116,818
−46,908	32,925	−53,987	40,431	−97,811	65,391	−100,224	73,150	−166,333	113,499	−161,777	119,354
−49,784	35,096	−57,295	42,968	−100,852	67,543	−100,533	75,685	−169,582	115,889	−165,066	121,889
−52,641	37,244	−60,604	45,505	−103,968	69,751	−106,842	78,220	−172,833	118,264	−168,396	124,425
−55,531	39,441	−63,913	48,042	−106,944	71,860	−110,152	80,755	−176,092	120,647	−171,705	126,960
−53,846	38,127	−60,604	45,505	−106,018	71,166	−106,842	78,220	−172,991	118,088	−168,396	124,425
−52,782	36,573	−57,295	42,968	−104,054	69,746	−103,533	75,685	−169,805	115,634	−165,086	121,889
−49,717	35,021	−53,987	40,431	−102,089	68,327	−100,224	73,150	−166,617	113,191	−161,777	119,353
−47,653	33,469	−50,678	37,894	−100,125	66,908	−96,915	70,615	−163,426	110,758	−158,468	116,818
−45,584	31,915	−47,370	35,356	−98,161	65,069	−93,605	68,081	−160,232	108,336	−155,158	114,283
−43,459	30,334	−44,062	32,819	−96,193	64,069	−90,296	65,546	−157,036	105,926	−151,849	111,747

Points located at the interface between the stone column and the surrounding soil

made in layers of 20 mm each. The sand layers were compacted by applying three different stresses: 11 kPa, 71 kPa and 135 kPa. Reinforced soil specimens were subjected to the same loading/unloading program (oedometer test method). The study is based essentially on the comparison of the effects on the void ratio. The approach, used in this study, is based on the replacement of the system formed by (soil-stone column) by an equivalent homogeneous soil

Table 7 Results of variation of deviatory stress q and effective mean stress p' according to the different loading–unloading phases

Point C		Point c		Point F		Point f		Point I		Point i	
Unit cell		Equiv Unit cell		Unit cell		Equiv Unit cell		Unit cell		Equiv Unit cell	
p' [kN/m²]	q [kN/m²]	p' [kN/m²]	q [kN/m²]	p' [kN/m²]	q [kN/m²]	p' [kN/m²]	q [kN/m²]	p' [kN/m²]	q [kN/m²]	p' [kN/m²]	q [kN/m²]
−38,832	28,603	−44,046	32,935	−87,404	58,005	−89,985	65,379	−154,882	104,424	−151,927	110,842
−41,770	30,818	−47,354	35,472	−91,229	60,665	−93,294	67,915	−158,618	107,290	−155,236	113,378
−44,669	33,025	−50,663	38,010	−94,336	62,825	−96,604	70,451	−161,908	109,759	−158,467	115,914
−47,596	35,255	−53,971	40,547	−97,384	64,957	−99,913	72,987	−165,120	112,124	−161,856	118,450
−50,526	37,489	−57,280	43,084	−100,412	67,081	−103,223	75,523	−168,318	114,467	−165,165	120,986
−53,485	39,746	−60,589	45,621	−103,516	69,257	−106,532	78,059	−171,525	116,824	−168,475	123,522
−56,391	41,962	−63,897	48,158	−106,481	71,347	−109,841	80,595	−174,713	119,141	−171,785	126,058
−55,087	40,967	−60,589	45,621	−105,529	70,529	−106,532	78,059	−171,864	117,153	−168,475	123,522
−53,114	39,460	−57,280	43,084	−104,054	69,072	−103,223	75,523	−168,838	114,999	−165,165	120,986
−51,142	37,954	−53,971	40,547	−103,560	67,616	−99,913	72,987	−165,812	112,848	−161,856	118,450
−49,170	36,447	−50,663	38,010	−101,591	66,161	−96,604	70,451	−162,784	110,699	−158,546	115,914
−47,195	34,939	−47,354	35,472	−99,622	64,705	−93,295	67,915	−159,755	108,553	−155,237	113,378
−45,199	33,416	−44,046	32,935	−97,679	63,246	−89,985	65,379	−156,724	106,410	−151,927	110,842

Points located at the outer limit of the unit cell

Table 8 Rates of variation (p') and (q): model of equivalent unit cell compared to the model of unit cell

Equivalent unit cell model-unit cell model)	Rate of variation					
	B-b	E-e	H-h	C-c	F-f	I-i
Effective mean stress p'	1%	0%	0%	1%	0%	0%
Deviatoric stress q	20%	10%	5%	10%	10%	5%

which has equivalent characteristics (equivalent void index e_{eq}). A comparison is made with the results of the case of a numerical study of the unit cell of stone column surrounding of soil. The unit cell is subjected to three different stresses: 50 kPa, 65 kPa, 80 kPa.

The evaluation of the new soil void index after installation of the column is obtained by the formula:

$$e = e_0 - \frac{\Delta V}{V_0}\left(1 + e_0\right) \tag{19}$$

or e_0, e: soil void index before and after installation of the column with: $\frac{\Delta V}{V_0} = \frac{\Delta e}{1+e_0}$. ΔV and Δe are the change in volume and the change in void index of the soil, respectively:

$$\Delta V = V_0 - V \text{ and } \Delta e = \left(e_0 - e\right) \tag{20}$$

The installation of the column induces variations in the cover ratio (a) and the void index (e) of the surrounding soil. These variations are related to the compaction stresses applied. From the calculated cover ratio (a) and void index (e) an initial equivalent void index of the equivalent homogeneous medium is determined using the formula:

Table 9 Effect of compacting stress

Compacting stress (kPa)	Experimental test		Compacting stress (kPa)	Numerical model	
	e/e_0	e_{eq0}/e_0		e/e_0	e_{eq0}/e_0
11	0.99	0.96	50	0.919	0.984
73	0.96	0.92	65	0.905	0.981
135	0.94	0.89	80	0.892	0.979

$$e_{eq0} = e_c a + (1 - a)e_s \tag{21}$$

e_c: index of voids of stone column after compaction; e_s: index of voids after installation of the column. The coverage rate (a) is determined by: $a = \frac{A_c}{A_s}$. A_c: surface of the column; A_s: surface of the soil.

Table 9 and Fig. 8 show the comparison between the experimental and numerical results variation of the initial void index ratio and the initial equivalent void index ratio as a function of compaction stresses in the laboratory model tests compared to those obtained from the numerical analysis of a unit cell. The both results show that the two ratios (e/e_0)

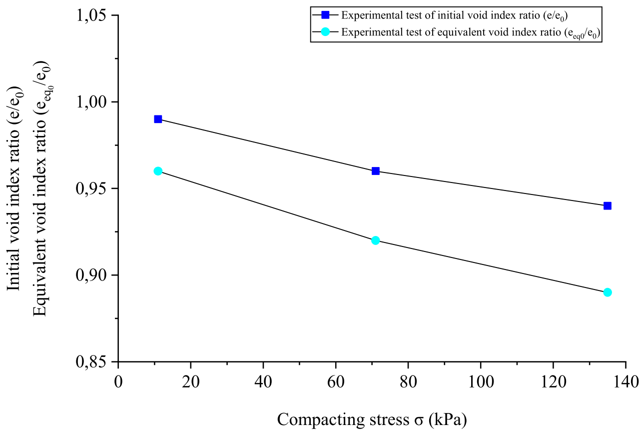

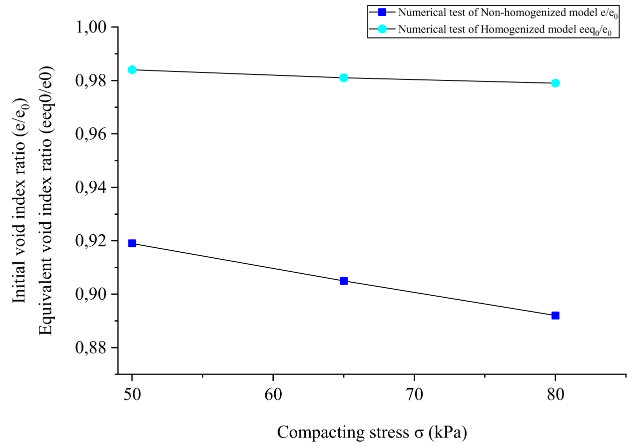

Fig. 8 Variation of ratios (e/e_0) and (e_{eq0}/e_0) of soil as a function of compaction stress

and (e_{eq0}/e_0) are inversely proportional to the compaction stress. Therefore, it can be observed that the void index of the soil and the equivalent void index decrease with increasing compaction stress of the stone columns.

6 Conclusion

This research study discusses two-unit cell models. The first model is a unit cell composed of stone column surrounded by loose soil. The second model is similar to the first, but it is homogeneous in terms of physical and mechanical parameters (equivalent materials).

For each model, a repartition mattress is preserved in the head of the stone column, which supports a concrete slab. Loading and unloading with an increment of 5 KN/m^2 applies to both models (loading of 50 KN/m^2 to 80 KN/m^2 unloading). An analysis is made in terms of void ratio variation and stress path variation. The points chosen for this analysis, some of them are in the stone column-soil interface and others on the outer boundary of the unit cells.

- The equivalent materials, thus introduced in second model seem to give results that led us to the following:
- The effect of overloading is significantly greater, as opposed to the stone column proximity effect at the interface of the column with the surrounding soil or at the end of the cell;
- The variation of the void ratio decreased by an average of 9% for the equivalent unit cell model compared to the model of stone column and soft soil unit cell;
- The stress trajectory of the equivalent model in this case clearly exhibits an increase of an average of 12% compared to the unit cell of stone column and loose soil;
- The model of equivalent unit cell, allows us to control results between loading and unloading phases. Which is not the case in the model of unit cell of stone column and loose soil.

The equivalent material applied to the second model illustrates in particular the difference between the behavior of processed and unprocessed soil. It is associated with the actual stresses existing in the soil and their evolution in time. However, the problem is not completely solved, as it remains related to some estimates such as the geometrical and mechanical characteristics of the stone columns and the initial state of the horizontal stresses in the soil.

More simulations and analyses will be required at a later stage to refine these results and to develop criteria for determining the values of these estimates more accurate. Finally, the unit cell models, thus investigated and the results obtained in this way could be compared with those of real cases. In this way, we could eventually confirm the efficiency of these equivalent parameters on the overall behavior of the structure.

Declarations

Conflict of interest The authors declare no competing interests.

References

Abdelkrim M, de Buhan P (2007) An elastoplastic homogenization procedure for predicting the settlement of a foundation on a soil reinforced by columns. Eur J Mech-A/Solids 26(4):736–757. https://doi.org/10.1016/j.euromechsol.2006.12.004

Babu MD, Nayak S, Shivashankar R (2013) A critical review of construction, analysis and behavior of stone columns. Geotech Geol Eng 31(1):1–22

Bouassida M, Carter J (2014) Optimization of design of column-reinforced foundations. Int J Geomech (ASCE) 14(6):04014031

Castro J (2017) Modeling stone columns. Materials 10(7):782. https://doi.org/10.3390/ma10070782

De Buhan P, Mangiavacchi R, Nova R, Pellegrini G, Salençon J (1989) Yield design of reinforced earth walls by a homogenization method. Geotechnic 39(2):189–201

Ellouse S, Bouassida M, Ben Salem Z, Znaidi MN (2016) Numerical analysis of the installation effects on the behaviour of soft clay improved by stone columns. Geomech Geoeng Int 12(2):73–85. https://doi.org/10.1080/17486025.2016.1164903

Gueguin M, de Buhan P, Hassen G (2013) A homogenization approach for evaluating the longitudinal shear stiffness of reinforced soil: column versus cross trench configuration. Int J Numer Anal Math Geomech 37:3150–3172. https://doi.org/10.1002/nag.2183

Gueguin M, Hassen G, de Buhan P (2015) Stability analysis of homogenized stone column reinforced foundations using a numerical yield design approach. Comput Geotech 64:10–19

Hadri S, Messat S, Bekkouche SR (2021) Numerical analysis of the performance of stone columns used for ground improvement. Jordan J Civ Eng 15(2):253–265

Hamzh A, Mohamad H, Bin Yusof MF (2019) The effect of stone column geometry on soft soil bearing capacity. Int J Eng 16(2):200–210. https://doi.org/10.1080/19386362.2019.1666557

Hassen G, De Buhan P, Abdelkrim M (2010) Finite element implementation of a homogenized constitutive law for stone column-reinforced foundation soils, with application to the design of structures. Comput Geotech 37(s1–2):40–49. https://doi.org/10.1016/j.compgeo.2009.07.002

Hassen G, Gueguin M, De Buhan P (2013) A homogenization approach for assessing the yield strength properties of stone column reinforced soils. Eur J Mech A/Solids 37:266–280

Jellali B, Bouassida M, De Buhan P (2005) A homogenization method for estimating the bearing capacity of soils reinforced by columns. Int J Num Anal Meth Geomech 29:89–1004. https://doi.org/10.1002/nag.441

Jellali B, Bouassida M, De Buhan P (2007) A homogenization approach to estimate the ultimate bearing capacity of a stone column reinforced foundation. Int J Geotech Eng 1:61–69. https://doi.org/10.3328/IJGE.2007.01.01.61-69

Killeen MM, McCabe BA (2014) Settlement performance of pad footings on soft clay supported by stone columns: a numerical study. Soils Found 54(4):760–776

Laouche M, Karech T, Rangeard D, Martinez J (2021) Experimental study of the effects of installation of sand columns in compressible clay using à reduced model. Geotech Geol Eng 39:2301–2312. https://doi.org/10.1007/s10706-020-01626-6(0123456789(),-volV()0123458697().,-vol

Maheshwari P, Khatri S (2012) Nonlinear analysis of infinite beams on granular bed-stone column-reinforced earth beds under moving loads. Soils Found 52(1):114–125

Nazir AK, Azzam WR (2010) Improving the bearing capacity of footing on soft clay with sand pile with/without skirts. Alex Eng J 49(4):371–377. https://doi.org/10.1016/j.aej.2010.06.002

Ng KS, Tan SA (2014a) Nonlinear behavior of an embankment on floating stone columns. Geoeng Geomech. https://doi.org/10.1080/17486025.2014.902118

Ng KS, Tan SA (2015) Simplified homogenization method in stone column designs. Soils Found 55(1):154–165. https://doi.org/10.1016/j.sandf.2014.12.012

Noui A, Karech T, Bouzid T (2019) A numerical investigation of dynamic behavior of a unit cell of a loose sand reinforced by stone column under the effect of gravity using Finn model. Indian Geotech J 49(3):255–264. https://doi.org/10.1007/s40098-018-0326-2

Schweiger HF, Pande GN (1986) Numerical analysis of stone column supported foundations. Comput Geotech 2:347–372

Shahrour I, Pruchinikcki E (1991). Application de la théorie de l'homogénéisation aux colonnes ballastées. Annales de l'institut technique du bâtiment et des travaux publics, 496, série sols et fondations. pp 118–128

Tabchouche S, Bouassida M, Mekki M (2019) Behavior of foundation on end-bearing stone columns group reinforced soil. Geotech Eng J SEAGS Et AGSSEA 50(4):71–77

Zeydi H, Boushehrian AH (2019) Experimental and numerical study of bearing capacity of circular footings layered soils with and without skirted sand piles. Iran J Sci Technol Trans Civ Eng 44(3):949–958. https://doi.org/10.1007/s40996-019-00284-w